J. Synchrotron Rad. (1995). **2**, 136–142

The Perfection of Protein Crystals Probed by Direct Recording of Bragg Reflection Profiles with a Quasi-Planar X-ray Wave

R. Fourme,[a]* A. Ducruix,[b] M. Ries-Kautt[b] and B. Capelle[a,c]

[a]LURE, CNRS-CEA-MESR, Bâtiment 209D, Université Paris-Sud, 91405 Orsay CEDEX, France, [b]Laboratoire de Biologie Structurale, CNRS-Université Paris-Sud, Bâtiment 34, 91198 Gif sur Yvette CEDEX, France, and [c]Laboratoire de Minéralogie et Cristallographie, CNRS-Universités Pierre et Marie Curie & Denis Diderot, 4 place Jussieu, 75252 Paris CEDEX 05, France

(Received 14 February 1995; accepted 16 March 1995)

Profiles of Bragg reflections from earth-grown crystals of lysozyme from hen egg-white and collagenase from *Hypoderma lineatum* were directly recorded with a quasi-planar X-ray wave. One crystal of each protein was chosen for a detailed investigation. Each sample is shown to consist of only a few (three and two, respectively) highly ordered domains, misoriented with respect to each other by a few arc seconds. The smallest rocking widths were observed for the large domain of the collagenase sample (FWHM corrected for instrumental broadening: 0.0016° for a strong reflection at 3 Å resolution). With appropriate improvements, this method might become a quantitative tool for characterizing the perfection of crystals from biological macromolecules.

Keywords: protein crystal perfection; crystal growth; lysozyme; collagenase.

1. Introduction

Growing high-quality crystals is a crucial step in the elucidation of the three-dimensional structure of biological macromolecules by X-ray diffraction methods. Physical chemistry is now routinely applied in the field of crystallogenesis (Chernov, 1993; Giegé, Lorber & Théobald-Dietrich, 1994) and efforts have been made to define criteria for crystal quality, in order to evaluate the effects of new methods such as growth in gels (Robert, Provost & Lefaucheux, 1992; Boué, Lefaucheux, Rosenman & Robert, 1993) or microgravity (Strong, Stoddard, Arrott & Farber, 1992; Trakhanov *et al.*, 1991). Two criteria are commonly used, based on the values of two parameters, maximum resolution and mosaic spread. The relation between these parameters is far from obvious, as discussed later.

The maximum resolution is the inverse value $d_{\min}$ of the largest value of the scattering vector modulus S ($S = 2\sin\theta/\lambda$) for which useful information on Bragg intensities can be extracted from a diffraction pattern recorded under given experimental conditions. Operational definitions of resolution are based either on the ratio $\langle I\rangle/\langle\sigma(I)\rangle$† in resolution shells or on values of $R_{\rm sym}$ (the relative disagreement between intensities of symmetry-equivalent reflections) as a function of S.

The mosaic spread η is a parameter associated with the mosaic crystal model commonly used to describe protein crystals. A mosaic sample is an assembly of a number of perfect domains (or blocks) slightly misoriented with respect to each other, and η is the extent of the angular misalignment of each domain with respect to every other domain. The overall sample reflecting width $\psi_{\mathbf{h}}$ of reflection **h** is a convolution of η with the intrinsic rocking width $\omega_{\mathbf{h}}$ of each domain ($\psi_{\mathbf{h}} > \omega_{\mathbf{h}}$; $\psi_{\mathbf{h}} = \omega_{\mathbf{h}}$ in the limiting case of a single-domain sample). In the case of reflection in the vertical plane of a unidirectional X-ray beam totally polarized in the horizontal plane, as used in the present experiments, the intrinsic rocking width $\omega_{\mathbf{h}}$, according to dynamical theory (Von Laue, 1960), can be expressed as

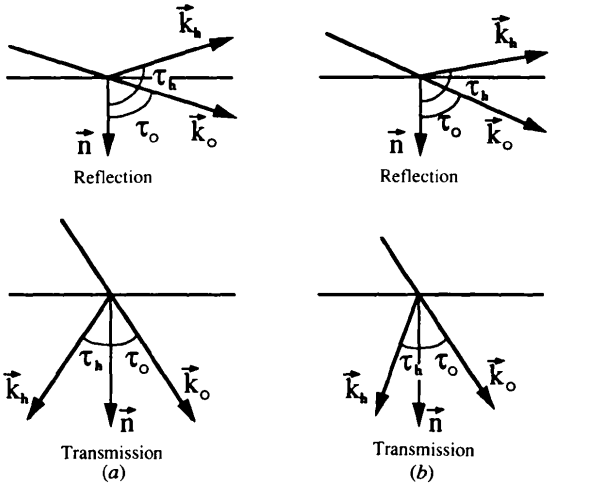

Figure 1
(*a*) Symmetric reflection in reflection and transmission. (*b*) Asymmetric reflection in reflection and transmission. Vectors and angles are defined in the text.

* To whom correspondence should be addressed.
† In this article, $\langle x\rangle$ is the root-mean-square value of x.

(in SI units):

$$\omega_{\mathbf{h}} = (2r_0/\pi)(\lambda^2/\sin 2\theta_B)(|F_{\mathbf{h}}|/V_0)|\gamma_{\mathbf{h}}|^{1/2}, \quad (1)$$

where r_0 is the classical electron radius ($r_0 = 2.82 \times 10^{-15}$ m), λ the X-ray wavelength, θ_B the Bragg angle, V_0 the volume of the crystal unit cell and $|F_{\mathbf{h}}|$ the structure-factor amplitude. $\gamma_{\mathbf{h}} = \cos(\mathbf{n},\mathbf{k_0})/\cos(\mathbf{n},\mathbf{k_h}) = \cos\tau_0/\cos\tau_{\mathbf{h}}$, where $\mathbf{n}$ is the normal to the crystal surface directed toward the interior of the crystal, and $\mathbf{k_0}$ and $\mathbf{k_h}$ are the wavevectors of the direct and diffracted X-ray beams, respectively (Fig. 1). $|\gamma_{\mathbf{h}}|$ is equal to 1 for a symmetric reflection ($\tau_0 = \tau_{\mathbf{h}}$) and greater or less than 1 for asymmetric reflections. The rocking width in the symmetrical case is denoted by $\omega_{s\mathbf{h}}$.

Assuming a (perfect single-domain) protein sample with typical unit-cell dimensions, ω values calculated on the basis of the dynamical theory are quite small, less than 1″ (Helliwell, 1988). The reason is that, for a primitive unit cell with n atoms and at a given resolution where the average (taking into account thermal motion) atomic scattering factor is $\langle f \rangle$, the average value $\langle |F| \rangle$ of structure amplitudes is proportional to $n^{1/2}\langle f \rangle$, whereas V_0 is roughly proportional to n, making $\langle |F| \rangle / V_0$ proportional to $\langle f \rangle / n^{1/2}$.

From (1), widths much larger than the average are expected for strong and asymmetric (with $|\gamma_{\mathbf{h}}| > 1$) reflections at low resolution. Widths are also dependent on the inverse unit-cell volume.

The experimental rocking width,* $\Phi_{\mathbf{h}}$, of a particular reflection is a convolution of $\psi_{\mathbf{h}}$ with the geometric and spectral parameters of the X-ray beam (Greenhough & Helliwell, 1982). Not surprisingly, over the last two decades decreasing experimental values of Φ have been reported for macromolecular crystals. This reduction is due essentially, if not exclusively, to improvements in collimation and monochromatization of X-ray beams, where the replacement of conventional X-sources by bending magnets or wigglers from electron/positron storage rings was essential [see Helliwell (1988) for a discussion of experimental results, and Colapietro *et al.* (1992)]. A further reduction has been observed with undulators, inserted in the magnetic structure of the ESRF at Grenoble, which provide a less-divergent X-ray beam (D. Stuart, personal communication). These observations suggest that experimental rocking widths for good macromolecular crystals are dominated by instrumental effects, and that the overall sample reflecting range, ψ, may be extremely small for some crystals. At least two experimental methods can be envisaged for estimating these widths, either a monochromatic beam with a rotating sample or a polychromatic beam with a stationary crystal (Laue method). In the Laue method (Helliwell, 1988), ψ values of individual reflections are derived from the radial extension of diffraction spots on the detector, after making various corrections including beam divergence, crystal-to-detector distance and detector point-spread function. The Laue method allows a fast survey of a very large number of reflections and is most suitable for comparing various samples (Weisgerber, 1993). We preferred the monochromatic method, because it can give accurate reflection profiles and is accordingly uniquely suited to the study of multidomain samples. We aimed at recording experimental rocking widths in conditions ensuring that instrumental effects have a small and parameterizable contribution to the experimental profiles, in order to find estimates of ψ values and, possibly, some insights into the hypothetical mosaic structure of the samples.

* In this article, width refers to the full width at half maximum (FWHM).

2. Materials and methods

2.1. *Samples*

Crystals from two proteins were used in these experiments: hen egg-white lysozyme (HEWL) in the tetragonal form and collagenase from fly larvae *Hypoderma lineatum* (CHL). HEWL is known to crystallize easily and has become a standard protein for protein crystal growth studies. CHL has been studied extensively (Carbonnaux, Ries-Kautt & Ducruix, 1995) by the team at Gif sur Yvette, and high-quality crystals can be grown routinely.

Triply crystallized HEWL (129 amino acids, empirical formula $C_{613}H_{952}N_{193}O_{185}S_{10}$) was obtained from Sigma (batch 54F-8155) and its purity was assessed by ion-spray mass spectrometry (molecular weight 14305 ± 2 Da). Sodium chloride (NaCl) and sodium acetate (NaOAc) (*pro analysi*) were purchased from Merck. Solutions in H_2O were prepared with commercially available deionized and triply distilled water for injectable preparation (Biosedra) and filtered through 0.22 µm filters. Crystals were obtained at 291 ± 0.1 K, using various conditions with 20–40 mg ml^{-1} lysozyme and 0.7–1 *M* NaCl in 50 m*M* NaOAc pH 4.5. The crystal space group is $P4_32_12$ with cell dimensions $a = b = 78.6$, $c = 37.8$ Å and eight molecules per unit cell. The resolution of data that can be recorded from these crystals is 1.3 Å, using synchrotron radiation from the wiggler beamline at LURE. The average temperature factor for this structure is $\langle B \rangle = 15$ Å^2.

CHL is a member of the collagenolytic enzymes related to the trypsin family. It cleaves native collagen in its helical part under physiological conditions of pH, temperature and ionic strength. It has collagenolytic activity in the midgut of the first instar migrating larvae from *H. lineatum* (Boulard, 1970). These larvae are endoparasites of cattle. The collagenase purified from *H. lineatum* larvae is a monomeric enzyme of molecular weight 25223 Da (230 amino-acid residues, empirical formula $C_{1128}H_{1715}N_{291}O_{350}S_8$). Crystals were obtained by vapour diffusion (Ducruix, Arnoux, Pascard, Lecroisey & Keil, 1981). As the enzyme does not suffer autolysis, crystallization could take place at neutral pH, close to optimal pH (8–8.5) for activity. Crystals were grown at 291 ± 0.1 K, and the best samples were obtained with a 20 mg ml^{-1} solution of CHL in 50 m*M* Tris pH 7.4 containing 60 m*M* NaCl and 1.23 *M* ammonium sulfate (note that crystallization was often hampered by twinning until NaCl was added). The crystal space group is *I*422 and the dimensions of the body-centred unit cell are $a = 111.7$ and $c = 165.8$ Å (32 molecules per unit cell). It is possible

to index reflections in a primitive triclinic cell with $a = b = 111.7$, $c = 114.5$ Å, $\alpha = \beta = 119.2$, $\gamma = 90.0°$. The resolution of data that can be recorded from CHL crystals using synchrotron radiation from the wiggler at LURE is 1.80 Å (Broutin, 1993). The average temperature factor for this structure is $\langle B \rangle = 24.5$ Å^2. Relatively large triangular-shaped crystals were selected, with overall dimensions of at least 400 µm.

Finally, four crystals of each protein were very carefully mounted in cylindrical Lindemann glass capillaries (diameter 1 mm) and sealed with wax in equilibrium with mother liquor. Experiments were performed at room temperature (293–294 K).

2.2. *Experimental set-up*

Experiments were performed at station D25b installed on beamline D2 of the positron storage ring DCI at LURE, a national synchrotron radiation facility at Orsay, France. The experimental set-up, designed and installed by the Laboratoire de Minéralogie et Cristallographie (Paris) with the primary goal of performing standing-wave experiments, features a double-crystal spectrometer with horizontal and parallel axis Δ_1 and Δ_2, two separate goniometric holders, and two slit collimators (Fig. 2). The first crystal, which rotates about Δ_1, acts as a monochromator. The second crystal is the sample itself, which can be rotated about the Δ_2 axis with either a stepping motor (fast scan) or a piezoelectric device (slow scan) giving steps of about 0.1″ with a dynamical precision of 0.01″. Intensities of beams diffracted by the sample are measured by an NaI scintillation counter mounted on an arm which can rotate about the Δ_2 axis. The sample is aligned on the Δ_2 axis. A high-resolution position-sensitive X-ray camera connected to a TV monitor is placed in the monochromatic beam. The magnified image of the crystal produced by this camera is due to differences in X-ray absorption by the crystal and its surroundings. With this camera, the sample holder could be accurately displaced in the vertical plane in order to have the sample either totally or partially irradiated. The entrance window of the scintillation detector was limited by

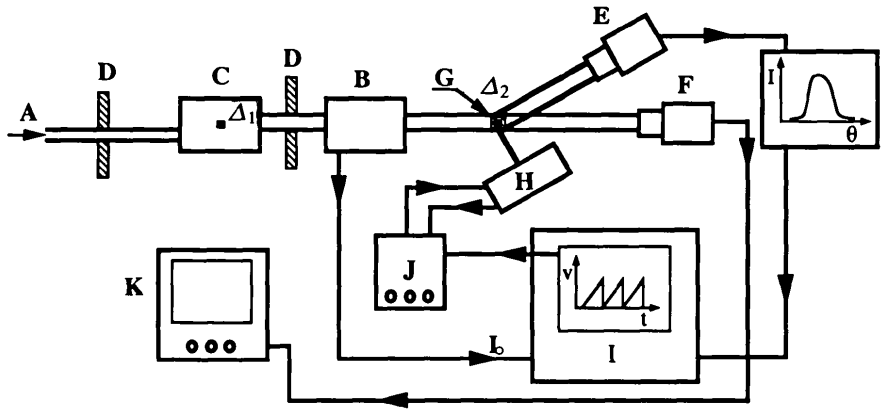

Figure 2
Principle of the experimental set-up. *A*: white X-ray beam. *B*: ionization chamber. *C*: monolithic monochromator. *D*: slits. *E*: scintillation counter. *F*: X-ray sensitive camera. *G*: sample. *H*: rotation and micro-angle measuring device. *I*: PC computer with data-acquisition board, slow angular scan drive, drift correction and beam intensity I_0. *J*: piezo drive. K: TV monitor. Δ_1 and Δ_2 are the horizontal axis of the monochromator and of the sample goniometric holder, respectively.

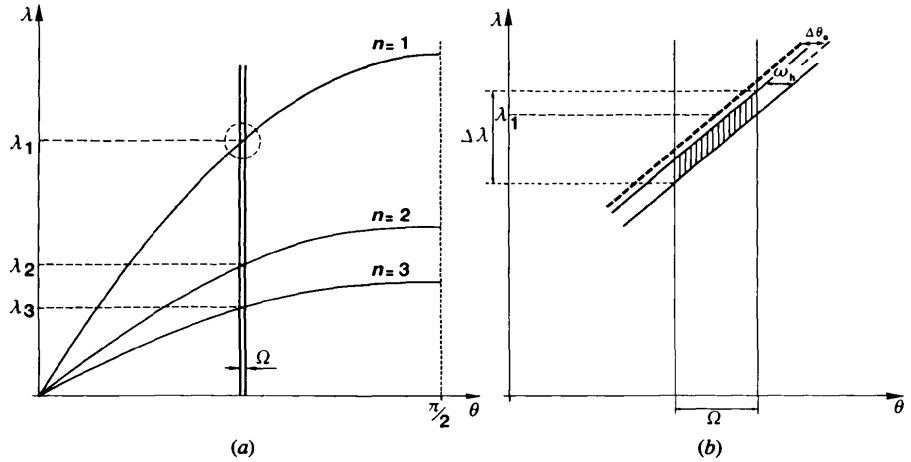

Figure 3
Principle of a DuMond diagram. (*a*) Curves $\lambda = f(\theta_B) = 2(d_h/n)\sin\theta_B$ with $n = 1$, 2 and 3. (*b*) Blow-up of the selected part of (*a*). Ω is the vertical divergence of the incoming beam, $\Delta\theta_0$ the correction to Bragg's law for refraction and ω_h the intrinsic rocking width of the reflection.

movable lead slits to about 1 × 1 mm^2. As the scintillation counter is not a position-sensitive detector, the selection of a diffracted beam from the protein crystal is performed as follows. The detector is set at a given $2\theta_B$ angle and then kept stationary. The crystal is rotated slowly and the output of the scintillation counter is recorded on a printer until a peak with a strong signal-to-noise is observed. Then, this peak is scanned repeatedly after displacing the detector slits by minute amounts, to ensure that only one reflection has been selected and its profile fully recorded. Finally, the rocking curve of the reflection is recorded with the computer-controlled piezoelectric device, accumulating 30 scans to improve counting statistics.

The vertical divergence Ω of the synchrotron radiation beam impinging on the monochromator is 15″ for 1 × 1 mm^2 slits. Specific monolithic crystal monochromators, with three symmetric and one asymmetric reflections, have been developed for this set-up (Boulliard *et al.*, 1992). They deliver a beam which approximates a plane wave. For the present work, an acceptable compromise between beam characteristics (divergence and bandpass) and intensity was found with an Si (220) crystal (Bragg spacing d = 1.9198 Å), oriented to reflect in the vertical plane. The wavelength was adjusted to λ = 1.23 Å (θ_B = 18.684°). At this wavelength, the rocking width of this monochromator is 0.37″ and the relative bandpass $d\lambda/\lambda$ is 5.3 × 10^{-6}.

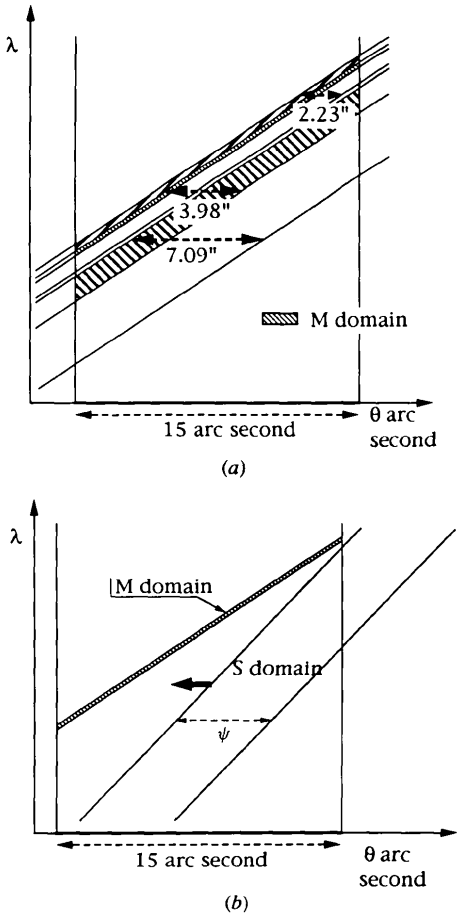

Figure 4
Principle of the derivation of the rocking curve using a DuMond diagram for (*a*) the multiple reflection monochromator, and (*b*) the monochromator–sample system.

The experimental width Φ_h of the rocking curve of a particular Bragg reflection, measured with this double-crystal spectrometer, will differ from the true sample rocking width ψ_h. This can be most conveniently discussed on the basis of a DuMond diagram (DuMond, 1937), which shows the domain (λ–θ) where crystalline diffraction occurs (Figs. 3*a* and 3*b*). To use such diagrams, it is convenient to define various angles pertinent to each reflection, with asymmetry $|\gamma|$, of the monochromator–sample system: ω_s (defined previously), the acceptance angle $\omega_i = |\gamma|^{-1/2}\omega_s$ and the divergence $\omega_r = |\gamma|^{1/2}\omega_s$ of the reflected beam. In the case of the monochromator used for this experiment, the first two reflections are symmetric, so that the corresponding domains on the DuMond diagram (Fig. 4*a*) are superimposed; they are limited by two vertical straight lines which correspond to the divergence Ω of the incident beam (15″) and by two lines parallel to the quasi-straight line $\theta_B(\lambda)$, separated by a distance equal to ω_s (3.98″). As the third reflection is asymmetric, the domains corresponding to the angular acceptance and to the divergence of the reflected wave are different (ω_i = 7.09″; ω_r = 2.23″). Finally, the narrow reflecting domain M of the monochromator is represented in Fig. 4(*a*), in which refraction has been accounted for. The experimental rocking curve of the sample is obtained by a displacement, parallel to the horizontal axis, of the domain S limited by two parallel straight lines separated by ψ, through domain M (Fig. 4*b*). The experimental rocking width is closest to ψ if the following two conditions are satisfied:

(i) The width of the M area is much smaller than ψ. As shown later, this condition is realised in this experiment.

(ii) The straight lines limiting the M and S domains are parallel, a condition which is obtained when the d values of the monochromator and the sample are equal. If not, the experimental profile is broadened.

A correction for the width of the M area and for the difference between monochromator and sample d values can be made to derive an estimate of the true value ψ from the experiment alone.

3. Results

Experiments were performed on four HEWL samples and four CHL samples. Because of the limited amount of time available at the synchrotron source, short tests were performed on all samples, and one crystal from each protein was chosen for a more detailed investigation. The lysozyme crystal was selected because fast scans of reflection profiles clearly suggested a composite structure, and the collagenase crystal because the profiles were the narrowest among those observed for the various samples.

3.1. *Lysozyme sample (A)*

Dimensions of this cube-shaped sample were close to 500 μm. The fast scan profile of a strong reflection at

2.8 Å resolution, shown in Fig. 5(*a*), is spread over *ca* 138″ and shows three main components separated by a few arc seconds plus additional secondary features. Three photographs of the Bragg spot were recorded on dental X-ray films (Kodak), adjusting the angular position of the crystal successively on the peak of each component (Figs. 6*a*–*c*). Each photograph is a topograph of a single crystal domain. The superposition of these three exposures on a fine-grain film (Kodak type M) reconstructs essentially the whole sample (Fig. 6*d*). After a vertical translation of the sample through the X-ray beam, using the TV monitor, only a large fraction of the largest domain was irradiated. The corresponding experimental rocking curve is a near-Gaussian single peak (Fig. 5*b*) with a width of 15.2″; the corrected width ψ is 14.5″ (0.0040°). From these observations, it can be concluded that this particular sample has a composite structure resulting from the association of essentially three highly ordered domains which are misoriented with respect to each other by a few arc seconds. The same experiment performed with a more divergent and/or less monochromatic beam, as used on a standard protein crystallography set-up, would have produced a single peak much larger than the individual components. Using the Laue method, Weisgerber (1993) has reported corrected rocking widths for tetragonal HEWL crystals: 0.0062 and 0.0032°, respectively, for two earth-grown crystals, and 0.0012 and 0.0010°, respectively, for two 'un-

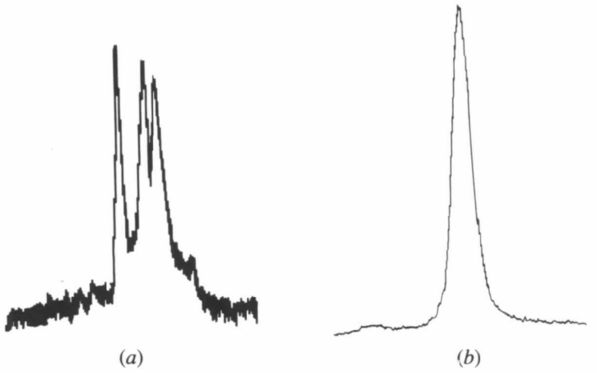

Figure 5
Experimental rocking width profiles for lysozyme sample *A* (single fast scan) obtained when illuminating (*a*) the whole sample and (*b*) the largest domain, corresponding to Fig. 6(*a*) (the two profiles are not on the same scale and the scan speeds were different).

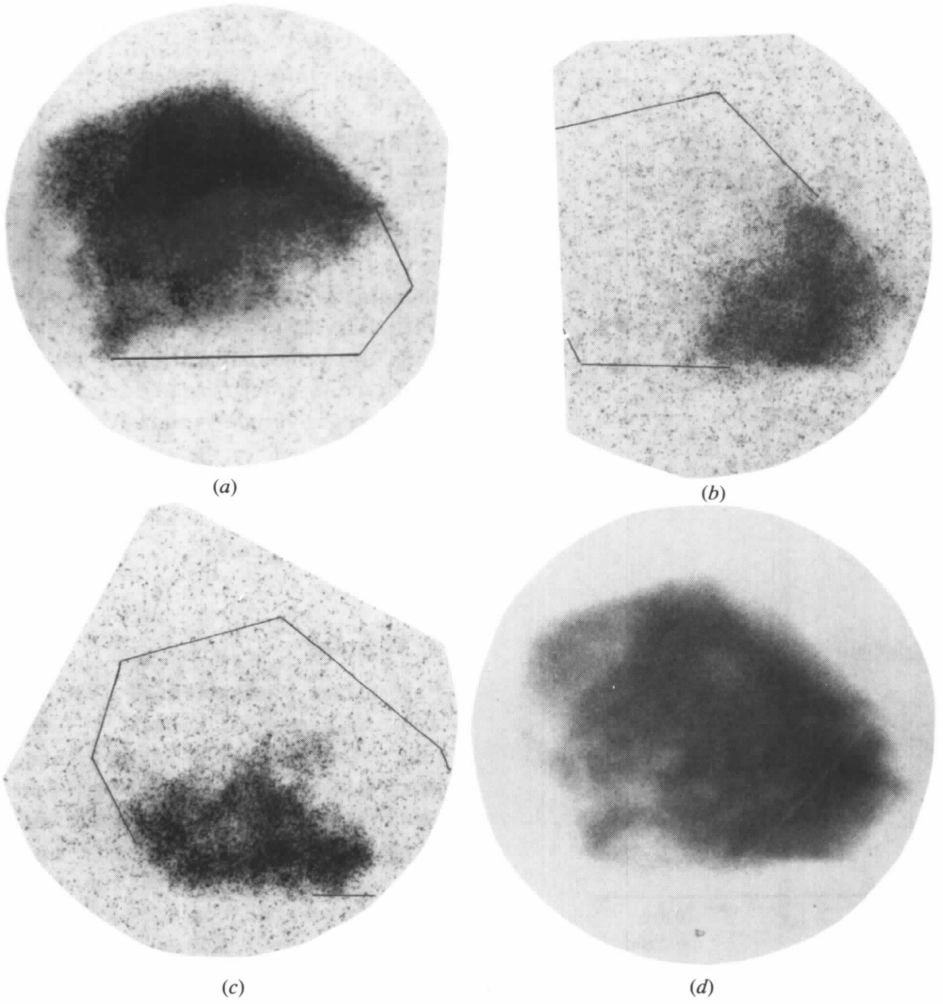

Figure 6
(*a*)–(*c*) Topographs of each of the three domains of lysozyme sample *A* recorded on dental film. (*d*) Superposition of the three previous topographs on a fine-grain film.

twinned' space-grown crystals. Estimates for those earth-grown crystals are in agreement with our earth-grown crystal results.

3.2. *Collagenase sample (B)*

Reflections of three out of the four collagenase samples had remarkably narrow profiles (< 12″). The sample producing the narrowest profiles was selected, with average dimensions close to 440 μm. The rocking curve of a strong reflection at 3 Å resolution from this sample was recorded over 30 slow scans. The superposition of two Gaussian components is sufficient to reproduce major features of the experimental profile, as shown in Fig. 7. The widths of these components are 7.8 and 15.6″. On the basis of the DuMond diagram for the five reflection monochromator–sample system, corrections have been applied to find estimated ψ values of 5.73 (0.0016) and 14.68″ (0.0041°), respectively.

Several other reflections were recorded, with similar profiles. The conclusion is that a single domain accounts for *ca* 75% of the sample volume, accompanied by one or several smaller domains with slightly different orientations.

4. Discussion

Finite dimensions of a crystal have an effect on the width of every reflection. The range of angles in the region of a maximum over which appreciable reflection occurs is of the order of the wavelength of the radiation used, divided by the linear dimension of the crystal fragment (James, 1948). At λ = 1.23 Å, for the large fragment of collagenase sample *B* with dimensions $\simeq$ 400 μm, this range is 0.06″. Accordingly, finite size effects can be neglected in the following discussion.

Assuming a hypothetical perfect collagenase crystal, equation (1) can be applied to obtain the theoretical rocking width ω of a symmetric 3 Å reflection, assuming a structure amplitude equal to the average structure amplitude $\langle|F|\rangle$. The result is ω = 0.005″. Even for an asymmetric ($|\gamma| > 1$) reflection with a very large structure amplitude (*e.g.* ten times larger than the average), ω would be *ca* 0.1″, whereas

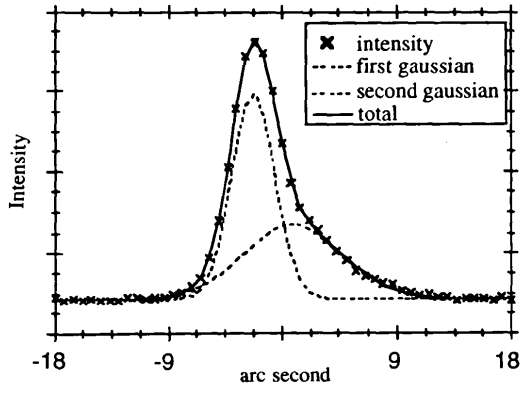

Figure 7
Experimental profile of a strong 3 Å reflection from collagenase sample *B* (30 slow scans) and its decomposition into two Gaussian components.

the ψ value estimated from the experimental results is 5.73″.

In conclusion, samples of both proteins have been found to have a composite structure with a limited number of coherent domains; in fact, it is likely that single-domain samples would be found by testing more samples. The ultra-small rocking widths obtained in this experiment indicate that these domains have an extremely good long-range order. The narrowest profiles were obtained for collagenase, but, even in this case, estimated ψ values are still significantly larger than values expected from dynamical theory. This discrepancy deserves further investigation:

(i) Experiments will be repeated with crystals grown under different conditions. Temperature changes during crystal transfers and data collection will be minimized. The sample manipulation will be improved. In particular, the use of flattened capillaries will be considered (Henderson, 1994), as cylindrical capillaries might induce mechanical stress distorting protein crystals.

(ii) The nature of lattice errors in macromolecular crystals is not fully understood, although discussions of this subject have appeared (Shaikevitch & Kam, 1981). The dimensions (up to several hundred micrometers) of domains observed in this experiment are sufficient for studies by X-ray topography. The photographs shown in Figs. 6(*a*–*c*) are indeed topographs of separate domains, but their contrast and spatial resolution are not sufficient to obtain solid information on possible extended defaults.

An interesting question is whether kinematical theory can be applied to an almost perfect domain, as protein crystallographers assume that $I_{\mathbf{h}} \propto |F_{\mathbf{h}}|^2$. The frontier between dynamical theory and kinematical theory is calculated from diffraction conditions and is called the extinction distance Λ, which can be defined in slightly different ways, but is of the order of (Becker, 1977):

$$\Lambda = (1/Cr_0)(V_0/|F_{\mathbf{h}}|\lambda) \qquad (2)$$

where C is the polarization factor and the other parameters are defined as in (1). For a crystal of thickness t, kinematical theory is valid if $\Lambda >> t$. Dynamical effects become appreciable when $\Lambda \simeq t$ (P. Becker, personal communication) and are very important for $\Lambda << t$. From (2), Λ is smallest for strong reflections and large wavelengths. Assuming that C = 1, λ = 0.9 Å (a wavelength commonly used in data collection with synchrotron radiation) and t = 300 μm, the minimum extinction distance $\Lambda_{\min}$ can be estimated and compared with t. For collagenase and tetragonal lysozyme, respectively, structure amplitudes have been calculated from the known atomic coordinates and temperature factors and then sorted out by decreasing values. The corresponding minimum extinction distances are *ca* 570 and 500 μm, so that primary extinction would be negligible for all reflections, even if domains diffracted as perfect crystals. Nevertheless, it may be advisable, especially for high-quality crystals with a small unit-cell volume, to estimate extinction distances in order to identify reflections that might be affected by primary extinction.

What is the potential impact of ultra-small rocking widths on the quality of diffraction data? Resolution depends on how the average intensity of Bragg reflections decreases with resolution down to the noise level, *i.e.* on the slope of the Wilson plot. Accordingly, resolution is primarily connected to short-range order in the crystal (Shaikevitch & Kam, 1981). As noted by these authors, the mosaic spread affects the maximum resolution only when $\psi \simeq d_{min}/a$, where a is the unit-cell linear dimension (*e.g.* for $d_{min} = 1$ Å and $a = 100$ Å, $\psi < 10$ mrad or 0.5°). Improving resolution for given crystals implies an increase of diffraction signals and a decrease of noise, which depends on the X-ray source, the detector, the experimental set-up and the data-collection method (Fourme, Bahri, Kahn & Bosshard, 1991). As discussed by Helliwell (1988), the signal-to-noise ratio can, in principle, be improved by a narrower rocking width; in practice, the finite rotation range in each diffraction image (typically 0.05° in the best cases, *i.e.* with fast readout detectors such as charge-coupled devices or proportional gas chambers) does not allow the full exploitation of this potential. Nevertheless, small rocking widths (if not smeared by instrumental effects) increase the number of reflections fully recorded in each image and reduce spatial overlaps between reflections.

The present experiments are only preliminary. In the short term, they will be pursued with the D25 instrument. Later, an improved experimental set-up is needed. Smearing by instrumental effects must be further reduced. This can be achieved by combining an undulator of the ESRF (Grenoble) and a narrow bandpass monochromator, producing an intense and almost planar X-ray wave. In addition, the flexibility of a four-circle diffractometer is required to determine sample orientation easily and select Bragg reflections for resolution, asymmetry and structure-factor amplitude. An instrument with a horizontal ω–2θ axis and the φ axis equipped with a piezoelectric device would be most appropriate. It will then be possible to record accurate profiles from wide to ultra-narrow reflections. Such measurements might become an effective tool for characterizing crystal perfection and evaluating the effects of various factors on this perfection.

The technical team of the DCI storage ring at LURE is acknowledged. We are grateful to J. R. Helliwell for sending us extracts from S. Weisgerber's PhD thesis. This work benefited from financial support from CNRS and the University of Paris-Sud; a grant from CNES (Centre National d'Etudes Spatiales) was allocated to AD's laboratory.

References

Becker, P. (1977). *Acta Cryst.* A**33**, 243–249.
Boué, F., Lefaucheux, F., Rosenman, I. & Robert, M. C. (1993). *J. Cryst. Growth*, **133**, 246–254.
Boulard, C. (1970). *C. R. Acad. Sci. Ser. D*, **270**, 1349–1351.
Boulliard, J. C., Capelle, B., Ferret, D., Lifchitz, A., Malgrange, C., Pétroff, J. F., Taccoen, A. & Zheng, Y. L. (1992). *J. Phys. (Paris) I*, **2**, 1215–1232.
Broutin, I. (1993). Thèse de Doctorat. Univ. of Paris-Sud, Orsay, France.
Carbonnaux, C., Ries-Kautt, M. & Ducruix, A. (1995). *Biophys. Chem.* Submitted.
Chernov, A. A. (1993). *Prog. Cryst. Growth Charact.* **26**, 121–151.
Colapietro, M., Cappucio, G., Marciante, C., Pifferi, A., Spagna, R. & Helliwell, J. R. (1992). *J. Appl. Cryst.* **25**, 192–194.
Ducruix, A., Arnoux, B., Pascard, C., Lecroisey, A. & Keil, B. (1981). *J. Mol. Biol.* **151**, 327–328.
DuMond, J. W. R. (1937). *Phys. Rev.* **52**, 872–883.
Fourme, R., Bahri, A., Kahn, R. & Bosshard, R. (1991). *Proceedings of the European Workshop on X-ray Detectors for Synchrotron Radiation Sources*, edited by A. H. Walenta, pp. 16–25. Center for Sensor Systems, Univ. of Siegen, Germany.
Giegé, R., Lorber, B. & Théobald-Dietrich, A. (1994). *Acta Cryst.* D**50**, 339–350.
Greenhough, T. J. & Helliwell, J. R. (1982). *J. Appl. Cryst.* **15**, 338–351.
Helliwell, J. R. (1988). *J. Cryst. Growth*, **90**, 259–272.
Henderson, S. J. (1994). *J. Appl. Cryst.* **27**, 1067.
James, R. W. (1948). *The Optical Principles of the Diffraction by X-rays*, pp 8–14. Woodbridge, Connecticut: Ox Bow Press.
Robert, M. C., Provost, K. & Lefaucheux, F. (1992). *Crystallization of Protein and Nucleic Acids: a Practical Approach*, edited by A. Ducruix & R. Giegé, p. 127. Oxford: IRL/Oxford Univ. Press.
Shaikevitch, A. & Kam, Z. (1981). *Acta Cryst.* A**37**, 871–875.
Strong, R. K., Stoddard, B. L., Arrott, A. & Farber, G. K. (1992). *J. Cryst. Growth*, **119**, 200–214.
Trakhanov, S. D., Grebenko, A. I., Shirikov, V. A., Gudkov, A. V., Egorov, V., Barmin, I. N., Vainstein, B. K. & Spirin, A. S. (1991). *J. Cryst. Growth*, **110**, 317–321.
Von Laue, M. (1960). *Röntgenstrahl-Interferenzen.* Frankfurt-am-Main: Akademische Verlag.
Weisgerber, S. (1993). PhD thesis, pp. 201–204. Univ. of Manchester, UK.